CORGI: Content-Rich Graph Neural Networks with Attention

Jooyeon Kim,[1*] **Angus Lamb,** [2] **Simon Woodhead,** [3] **Simon Peyton Jones,** [2] **Cheng Zheng,** [2] **Miltiadis Allamanis** [2]

[1] RIKEN, Japan
[2] Microsoft Research, Cambridge, UK
[3] Eedi, UK

Abstract

Graph representations of a target domain often project it to a set of entities (nodes) and their relations (edges). However, such projections often miss important and rich information. For example, in graph representations used in missing value imputation, items — represented as nodes — may contain rich textual information. However, when processing graphs with graph neural networks (GNN), such information is either ignored or summarized into a single vector representation used to initialize the GNN. Towards addressing this, we present CORGI, a GNN that considers the rich data within nodes in the context of their neighbors. This is achieved by endowing CORGI's message passing with a personalized attention mechanism over the content of each node. This way, CORGI assigns *user-item-specific* attention scores with respect to the words that appear in an item's content. We evaluate CORGI on two edge-value prediction tasks and show that CORGI is better at making edge-value predictions over existing methods, especially on sparse regions of the graph.

Introduction

Graph neural networks (GNN) have enjoyed great success in deep learning. GNNs allow us to model complex graph-structured data. However, the construction of the input graphs is often a lossy projection of the data of the modeled domain. For example, a graph representation of a book recommendation problem may represent books and users as nodes with valued edges as recommendations. However, each book node contains rich semi-structured content, such as text structured into sections, tables, etc., which can be used to improve the performance of recommendations.

A common approach to incorporate node content in GNNs is to "summarize" it into a single vector representation (embedding) and use the vector as an initial node embedding. This often includes computing a single vector representation from a whole sentence or document using an encoder model, such as a bag-of-words model or a transformer. However, such representations are suboptimal, given the relatively small size of these vectors compared to the original content. This is widely accepted in natural language processing (NLP), and instead of representing inputs as a single vector/embedding, the full input is used. For example, encoder-decoder models employ some form of attention

mechanism over the whole input given the model context instead of representing it as a single vector. For example, in NLP text summarization (You et al. 2019), a decoder attends to the encoded representations of all the words in the input text.

In the same fashion, we need a better way for a GNN to capture the content within nodes of a graph. Towards this goal, we present CORGI (Content-Rich Graph neural network with attention), a message-passing GNN (Gilmer et al. 2017) that incorporates an attention mechanism over the rich *node* content during each message passing step. This allows CORGI to effectively learn *both* about the structure of the graph and the content within each node.

One interesting application of CORGI is edge-value imputation, e.g., missing value imputation with GNNs in collaborative filtering (You et al. 2020) (Fig. 1-left). For example, in a dataset of student-question answers, each question is associated with a rich textual description. In such settings, graph-based representations capture the rich interactions among students and questions (user responses) but ignore important content within items (textual descriptions of questions; text in Fig. 1). CORGI combines both sources of information through a personalized attention-based message passing method that computes user-item (student-question) pair-specific representations of the item's content. Additionally, CORGI achieves better performance compared to baselines, particularly in sparse regions of the user-item graph, such as rarely answered questions.

Contributions In summary, our contributions are • CORGI: a message-passing GNN that incorporates an attention mechanism over node content during messages computation. • A specialization of CORGI for the user-item recommendation. • An extensive evaluation over two real-world datasets showing that CORGI improves user-response prediction performance over existing methods, especially for items with few user ratings or in sparse graphs, where content plays a critical role.

CORGI Architecture

In this section, we first describe CORGI's problem setting and its implementation. We then focus on the recommender systems use-case with textual content in item nodes. Finally, we discuss CORGI's computational complexity and how to
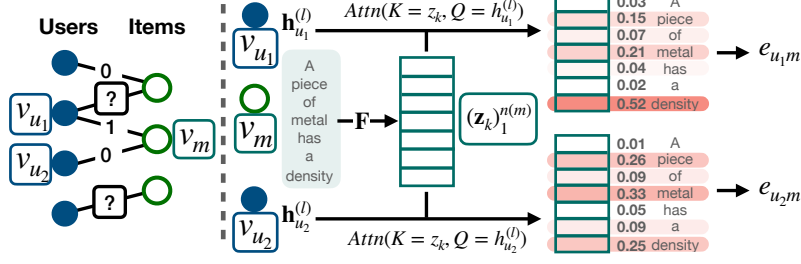

Figure 1: **Left**: In an educational setting, students (users) and questions (items) form a bipartite graph. Predicting student responses can be posed as missing edge value imputation. Edge values are known for some user-item pairs but not for all. **Right**: The edge representation computation in CORGI's lth message-passing layer. Item nodes are associated with content (e.g., a question node v_m contains text). The node content is encoded by a model $\mathbf{F}$ (e.g., a transformer), obtaining a set of content vectors $\mathbf{Z_m} = \{\mathbf{z}_k\}_1^{n(m)}$. During message passing, CORGI computes the representation of an edge (e.g., $\mathbf{e}_{u_1 m}$) using the last layer's node embedding of a user (student) node (e.g., $\mathbf{h}_{u_1}^{(l)}$) and an attention mechanism over $\mathbf{Z_m}$. Thus, message passing takes into consideration the full content within the item (question) nodes in a personalized user-dependent way.

Algorithm 1: CORGI message-passing computation

1 **for** $l \in \{1, \dots, L\}$ **do**
2   **for** $i \in \mathcal{V}$ **do**
3        $\mathbf{m}_{ij}^{(l)} \leftarrow$ Compute messages from Eq. 1 ;
4        $\mathbf{h}_i^{(l)} \leftarrow$ Update node states with Eq. 2 ;
5   **for** $v_j \in \mathcal{N}(i)$ **do**
6           $c_{ik}^{(l)} \leftarrow$ Compute CA scores from Eq. 6 or Eq. 7 ;
7           $\alpha_{ik}^{(l)} \leftarrow$ Compute content attention probability from Eq. 5 ;
8           $\mathbf{e}_{ij}^{(l)\prime} \leftarrow$ Update content-independent edge embedding with Eq. 3 ;
9           $\mathbf{e}_{ij,\text{CA}}^{(l)} \leftarrow$ Update content-attention edge embedding with Eq. 4 or use cache;
10           $\mathbf{e}_{ij}^{(l)} \leftarrow \mathbf{e}_{ij}^{(l)\prime} + \mathbf{e}_{ij,\text{CA}}^{(l)}$

Output: Node embeddings $\mathbf{h}_v, \forall v \in \mathcal{V}$

---

reduce it. The appendix summarizes our notation.

Problem setting Consider a graph $\mathcal{G} = (\mathcal{V}, \mathcal{E})$. Each node $v \in \mathcal{V}$ is associated with node features $\mathbf{h}_v^{(0)}$ and each edge with the features $\mathbf{e}_{ij}^{(0)}, \forall (i, j) \in \mathcal{E}$. If a node or edge is *not* related with any features, a constant value may be assigned. A subset of nodes $\mathcal{V}_C \subset \mathcal{V}$ is associated with a set of $n(i)$ *content* vector representations $\mathbf{Z}_i = \{\mathbf{z}_1^{(i)}, \dots, \mathbf{z}_{n(i)}^{(i)}\}, \forall v_i \in \mathcal{V}_C$, and $\mathbf{z}_k^{(i)} \in \mathbb{R}^D$. Notice that $n(i)$, the number of content vectors of each node v_i, may differ. $\mathbf{Z}_i$ may be given or computed with a node content encoder (e.g., a transformer).

CORGI The goal is to learn representations over the nodes while considering both the graph structure and the set of content vectors within each node (Fig. 1). CORGI follows the message-passing GNN paradigm (Gilmer et al. 2017) and is closely related to GRAPE (You et al. 2020). In

contrast to existing models, CORGI uses the content vector representations associated with each node during message-passing with personalized attention. Specifically, CORGI computes messages by learning to focus on potentially different parts of the content in the context of the neighboring nodes using an attention mechanism (Fig. 1). Alg. 1 presents a high-level overview of CORGI, discussed next.

CORGI's architecture assumes L message passing layers. Following You et al. (2020), at each layer l, CORGI computes a *message* $\mathbf{m}_{ij}^{(l)}$ from node v_j to v_i using the previous-level node embedding $\mathbf{h}_i^{(l-1)}$ and edge embedding $\mathbf{e}_{ij}^{(l-1)}$ as

$$\mathbf{m}_{ij}^{(l)} = \sigma \left(\mathbf{P}^{(l)} \cdot \left[\mathbf{h}_j^{(l-1)}, \mathbf{e}_{ij}^{(l-1)} \right] \right), \quad (1)$$

where σ is a non-linearity, $[\cdot]$ is vector concatenation, and $\mathbf{P}^{(l)}$ is a trainable weight. We set $\mathbf{h}_i^{(0)}$ and $\mathbf{e}_{ij}^{(0)}$ to the input node features and input edge attributes (if any), and $\mathbf{h}^{(l)} \in \mathbb{R}^{C^{(l,h)}}$, $\mathbf{e}^{(l)} \in \mathbb{R}^{C^{(l,e)}}$. Messages are *aggregated* from all neighbors $\mathcal{N}(i)$ of v_i and node embedding are *computed* as

$$\mathbf{h}_i^{(l)} = \sigma \left(\mathbf{Q}^{(l)} \cdot \left[\mathbf{h}_i^{(l-1)}, \text{AGG}^{(l)} \left(\mathbf{m}_{ij}^{(l)} \mid \forall j \in \mathcal{N}(i) \right) \right] \right), \quad (2)$$

where $\text{AGG}^{(l)}$ is a permutation-invariant aggregation function, and $\mathbf{Q}^{(l)}$ is a learnable parameter.

We are interested in incorporating information from the content of each node $v_j \in \mathcal{V}_C$. To achieve this, we use an attention mechanism within the GNN's message-passing. This allows a message between a v_i and v_j to *focus* on a specific part of the content. Such an ability can be helpful in many scenarios. For example, in an educational recommender system, the attended (textual) content of a question is an essential factor in predicting the student's ability to answer it correctly given, e.g., a diagnostic question (Wang et al. 2020). Intuitively, a student — given her skills — will focus on different aspects of a question when answering it.

CORGI's attention mechanism aims to emulate this. To model this, we combine any edge features $\mathbf{e}_{ij}^{(0)}$ with a content-attention vector $\mathbf{e}_{ij,\text{CA}}^{(l)}$ computed from an attention

mechanism over the content $\mathbf{Z}_{v_j}$. We consider two options for this: (a) element-wise addition $\mathbf{e}_{ij}^{(l)} = \mathbf{e}_{ij}^{(l)\prime} + \mathbf{e}_{ij,\text{CA}}^{(l)}$, and (b) concatenation $\mathbf{e}_{ij}^{(l)} = \left[\mathbf{e}_{ij}^{(l)\prime}, \mathbf{e}_{ij,\text{CA}}^{(l)}\right]$, where

$$\mathbf{e}_{ij}^{(l)\prime} = \sigma\left(\mathbf{W}^{(l)} \cdot \left[\mathbf{h}_j^{(l)}, \mathbf{e}_{ij}^{(0)}\right]\right), \qquad (3)$$

with a trainable weight $\mathbf{W}^{(l)}$, and $\mathbf{e}_{ij,\text{CA}}^{(l)}$ is computed by the attention mechanism, discussed next. Note that for element-wise addition $\mathbf{e}_{ij}^{(l)\prime}$ must have the same cardinality as $\mathbf{e}_{ij,\text{CA}}^{(l)}$.

Finally, we describe the attention mechanism computing $\mathbf{e}_{ij,\text{CA}}^{(l)}$. For an edge between v_i and v_j at l^{th} layer, the content-attention (CA) is computed using the set of content vector representations of v_j, $\mathbf{Z}_j$, and the previous-level node embedding $\mathbf{h}_i^{(l-1)}$, i.e.,

$$\mathbf{e}_{ij,\text{CA}}^{(l)} = \text{ATTENTION}\left(\text{KEYS} = \mathbf{Z}_j, \ \text{QUERY} = \mathbf{h}_i^{(l-1)}\right)$$
$$= \sum_k \alpha_{ik} \mathbf{W}_M^{(l)} \mathbf{z}_k^{(v_j)}$$
$$(4)$$

where $\mathbf{W}_M^{(l)}$ is a trainable weight, and α_{ik} is computed as

$$\alpha_{ik}^{(l)} = \text{SOFTMAX}_k\left(c_{ik}^{(l)} \mid \forall k \in \{1, \dots, n(i)\}\right). \quad (5)$$

We test two common mechanisms for computing $c_{ik}^{(l)}$: concatenation (CO) and dot-product (DP), computed as

$$c_{ik,CO}^{(l)} = \sigma\left({\mathbf{p}^{(l)}}^\top \left[\mathbf{W}_U^{(l)} \mathbf{h}_i^{(l-1)}, \mathbf{W}_M^{(l)} \mathbf{z}_k\right]\right) \qquad (6)$$

$$c_{ik,DP}^{(l)} = \sigma\left(\left[\mathbf{W}_U^{(l)}, \mathbf{h}_i^{(l-1)}\right]^\top \mathbf{W}_M^{(l)} \mathbf{z}_k\right), \qquad (7)$$

where $\mathbf{W}_U^{(l)}$, and $\mathbf{p}^{(l)}$ are learnable weights. Note that the attention is over the node content and should not be confused with the attention used in GATs (Veličković et al. 2018). We provide a detailed explanation in the related work section.

Content representations So far, we assumed that the content representation vectors $\mathbf{z}_j^{(v_i)} \in \mathbb{R}^D$ are given. In practice, these representations can be computed from some deep learning component $\mathbf{F}$. CORGI does *not* impose a structure on $\mathbf{F}$. For example if the node content is images, then CNN-based architectures for $\mathbf{F}$ would be reasonable. Similarly, if the content is text, i.e., a sequence of words (or any other sequence), then any NLP model can be used. This includes text representation models (Bojanowski et al. 2017; Mikolov et al. 2013; Pennington, Socher, and Manning 2014) and sequence encoders (Cho et al. 2014; Peters et al. 2018; Sutskever, Vinyals, and Le 2014), including transformers (Devlin et al. 2019; Vaswani et al. 2017). Such models "contextualize" each individual word in the sequence and convert it to a *set* of vector representations.

CORGI for user-response prediction

User response prediction can be formulated as an edge-value prediction (Berg, Kipf, and Welling 2017; Wang et al. 2019;

You et al. 2020; Zhang and Chen 2020). We operationalize CORGI for recommender systems by considering a *bipartite* graph $\mathcal{G} = (\mathcal{V}, \mathcal{E})$ with two disjoint node sets $\mathcal{V} = \mathcal{V}_U \cup \mathcal{V}_M$ of users and items. Each item $v_m \in \mathcal{V}_M$ contains text $\mathbf{D}_m = \left[w_1^{(m)}, \cdots, w_{n(m)}^{(m)}\right]$, i.e., a sequence of words. The sequence is converted to a set of content vectors $\mathbf{Z}_m$ using a sequence encoder and is input to CORGI. An edge value prediction, i.e., a recommendation $r(v_m, v_u)$ for a user v_u about an item v_m is made with a read-out layer, defined as

$$r(v_m, v_u) = \sigma\left(\mathbf{w}_{\text{out}}^T \left[\mathbf{h}_u^{(L)}, \mathbf{h}_m^{(L)}\right] + b\right), \qquad (8)$$

where $\mathbf{w}_{\text{out}}$ and b are learnable weights.

Complexity analysis

CORGI's computational and memory complexity is similar to most message-passing GNNs, with the additional cost of the attention mechanism. Compared to the node-to-node attention of GATs, CORGI's attention mechanism involves maximum of $T = \max_{v \in \mathcal{V}_M}(|\mathbf{Z}_v|)$, the maximum content size with respect to $v \in \mathcal{V}_C$, for each content node. For the lth message-passing CORGI layer the computational complexity for computing the content attention is expressed as:

$$\mathcal{O}\Big(|\mathcal{V}_U| \cdot C^{(l-1,h)} \cdot C^{(l,e)} + |\mathcal{V}_M| \cdot T \cdot D \cdot C^{(l,e)}$$
$$+ |\mathcal{E}| \cdot T \cdot C^{(l,e)}\Big), \qquad (9)$$

The first and the second terms arise from the multiplication between the trainable weights and the node embeddings or content vector representations, in Eq. 6 or 7. The last term is due to the pairwise linear operation in the attention coefficient calculation between the queries and keyes, in Eq. 4.

We can drastically reduce the complexity by using the neighbor sampling method proposed by Hamilton, Ying, and Leskovec (2017) and caching all $\mathbf{e}_{ij,\text{CA}}^{(l)}$. For network sampling, we sample a subset of nodes $\mathcal{V}' = \left\{\mathcal{V}_U' \cup \mathcal{V}_M'\right\}$ for the neighbor sampling and only update $\mathbf{e}_{ij,\text{CA}}$ whose target node v_j is in $\mathcal{V}_M'$ and source node v_i is in $\mathcal{N}(\mathcal{V}_M')$. The sampled subgraph is $\mathcal{G}' = \left\{\mathcal{V}'', \mathcal{E}'\right\}$, with $\mathcal{V}'' = \left\{\mathcal{V}_M' \cup \mathcal{N}(\mathcal{V}_M')\right\}$. This way, the computational cost is reduced.

Computing the attention for each layer is costly both in terms of memory and computation. To drastically reduce the memory and compute requirements, we use a caching trick for all $\mathbf{e}_{ij,\text{CA}}^{(l)}$. Since these representations can be thought as edge features, we want to compute them infrequently and re-use them. To do this, we create a cache for all $\mathbf{e}_{ij,\text{CA}}^{(l)}$ and initialize them with zeros. Then, at the final layer L, we compute $\mathbf{e}_{ij,\text{CA}}^{(L)}$ using Eq. 4 and update the cache for all $\mathbf{e}_{ij,\text{CA}}^{(l)}$ to the computed $\mathbf{e}_{ij,\text{CA}}^{(L)}$. The newly cached values will be used in subsequent message-passing iterations. In this way, we avoid $L-1$ computations of Eq. 4.

Related work

CORGI is at the intersection of GNNs and machine learning models for missing value imputation. Related work that is used as baselines in the evaluation is *emphasized*.

Missing value imputation is the task of filling in previously unknown entries with predicted values. For two heterogeneous groups, namely, users and items, the task is commonly reduced to matrix completion (Bennett, Lanning et al. 2007) with numerous collaborative filtering and matrix factorization approaches (Billsus, Pazzani et al. 1998; Koren, Bell, and Volinsky 2009; Linden, Smith, and York 2003; McAuley and Leskovec 2013; Mnih and Salakhutdinov 2007; Sarwar et al. 2001) and deep learning-based approaches (Spinelli, Scardapane, and Uncini 2020; Vincent et al. 2008; Yoon, Jordon, and Schaar 2018). *Deep matrix factorization (DMF)* (Xue et al. 2017) directly uses the input matrix by feeding this information through multilayer perceptrons (MLPs). An extension to variational autoencoders (VAE) (Kingma and Welling 2014), the *partial-VAE model (PVAE)* (Ma et al. 2019) is an encoder-decoder-based approach for imputing missing values. In contrast, CORGI leverages additional content information in a user-item-specific manner through attention in message-passing.

Over the past years, there have been attempts to model graphs (Grover and Leskovec 2016; Perozzi, Al-Rfou, and Skiena 2014; Tang et al. 2015). Kipf and Welling (2017) proposed *graph convolutional networks (GCNs)*, a neural network that learns latent representations of nodes, amongst other deep neural network-based approaches (Bruna et al. 2013; Defferrard, Bresson, and Vandergheynst 2016; Duvenaud et al. 2015; Li et al. 2016; Niepert, Ahmed, and Kutzkov 2016; Scarselli et al. 2008). *GraphSAGE* (Hamilton, Ying, and Leskovec 2017) extends GCNs allowing the model to be trained on some part of the graph, enabling inductive learning settings. *Jumping knowledge (JK)* network (Xu et al. 2018) and *Graph Isomorphism Network (GIN)* (Xu et al. 2019) are proposed to improve the representation power of GNNs by adopting new aggregation schemes with respect to the representations of different layers and their previous representations. A GNN model that is designed for recommender systems, *graph convolutional matrix completion (GC-MC)* (Berg, Kipf, and Welling 2017) is a variant of GCNs that explicitly uses edge labels as inputs to model messages. Compared to other approaches, GC-MC employs a single-layer message-passing scheme, and each label is endowed with a separate message passing channel. *GRAPE* (You et al. 2020) employs edge embeddings on GCNs and adopts edge dropout applied throughout all message-passing layers. LightGCN (He et al. 2020) designs a GCN framework that simplifies or omits constructions that are not beneficial for recommendations, such as feature transformation and nonlinear activation, and puts more emphasis on neighborhood aggregation. Compared to the previously proposed GNN models in recommender systems, CORGI leverages the rich content information of nodes to model a target domain projected to graphs. Compared to existing GNN models that exploit the content information of nodes, CORGI employs an attention mechanism over node content within the GNN's message-passing and computes user-item-specific attention which is used to update edge embeddings. Wu et al. (2020) surveys the recent literature on GNNs for recommender systems.

In natural language processing, the (self-)attention is used to relate word or word tokens of a given sequence (Lin et al. 2017; Parikh et al. 2016; Paulus, Xiong, and Socher 2018; Vaswani et al. 2017). Many GNN models (Gao and Ji 2019; Hou et al. 2020; Kim and Oh 2021; Zhang et al. 2018), with *graph attention networks (GATs)* (Veličković et al. 2018) being a popular example, use an attention mechanism to allow the target nodes to distinguish the weights of multiple messages from the source nodes for aggregation. We note that CORGI is orthogonal to the GAT-like models; although CORGI uses attention, it is over the content within each node instead of the neighbors of each node (as in GATs). In future work CORGI-like mechanisms can be embedded to GAT-like GNNs.

Evaluation

Model configuration   We employ the $L = 3$ CORGI with node embedding and edge embedding cardinalities $C^{(l,h)}$ and $C^{(l,e)}, \forall l \in \{1, \dots, L\}$ set to 64, and size of the prediction read-out layer in Eq. 8 is set to 256. We initialize node embeddings to random values, and assign the train label values to initialize the edge embeddings. We use mean pooling for aggregation. For the non-linear activation, we use LeakyReLU for attention coefficient computation (Eq. 6, 7) with negative slope set to 0.2, as suggested by Veličković et al. (2018) and ReLU (Nair and Hinton 2010) for the rest.

Training configuration   For all experiments, we train CORGI with Adam (Kingma and Ba 2014) and a learning rate of 0.001. We employ early stopping on validation loss, with train, test, and validation sets split in 8:1:1 ratio. We use binary cross entropy loss (BCE) for binary values and mean squared error (MSE) for ordinal values. We apply dropout (Srivastava et al. 2014) on the message passing layers, the prediction MLPs, as well as on edges, with rates chosen from {0.1, 0.3, 0.5, 0.7} with respect to the validation set performance. For the baselines, the parameter settings are done in the following manner: 1) When the settings of the comparison models overlap with CORGI's, e.g., the number of message passing layers or the learning rate, we used the same configurations as CORGI. 2) For the parameter settings that are unique to the comparison model, we followed the setting that is disclosed in the original paper. 3) When the setting disclosed in the original paper is not applicable to the datasets used or our training environment, we select those that yield the best validation performance.

Synthetic experiments

First, we create a synthetic dataset to validate our model design. We create a random bipartite graph with item and user nodes. Each item-node is associated with a number of "words" as its content. We use a "vocabulary" of 5 words and each item node contain each of the 5 words with 50% probability. Each user-node is assigned a single *focus word* that indicates the word the user "likes". Finally, the value of an edge between a user and an item is deterministically set to 1 if the item contains the user's "focus word", and 0 otherwise. Throughout experiments, the word-content of items is provided as an input to CORGI, but the user focus word is latent. We are interested in understanding if CORGI
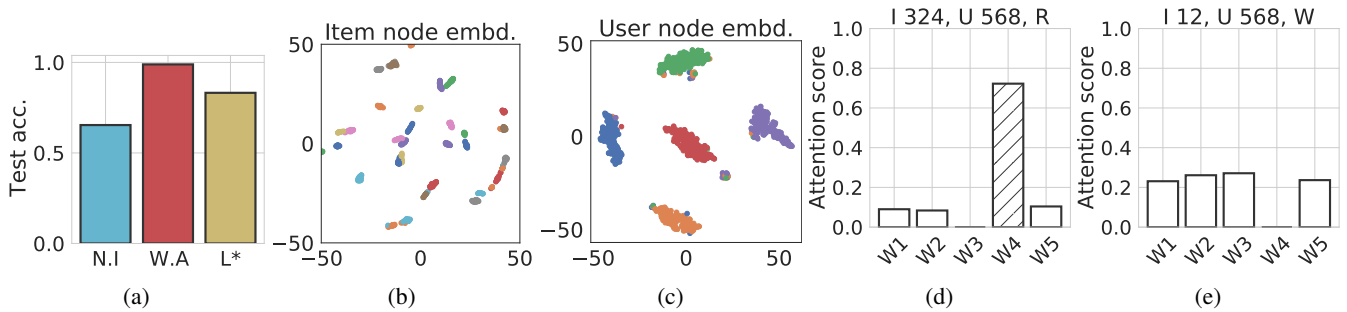
Figure 2: Synthetic experiment results. (a): Test accuracies when using item content information for node initialization (N.I.), for computing content attentions (W.A.), and when the the edge labels are given (L*). (b), (c): t-SNE plots of learned item and user node embeddings using CORGI. Each dot represents a single node and is colored by its word distribution (item) and word-attentiveness (user). (d), (e): Computed word-attention scores of a user with correct and incorrect answers.

can predict the correct edge labels between users and items, which can easily be achieved using content. Furthermore, by inspecting attention scores, we analyze CORGI's ability to learn to focus on the user's focus word within each item node, if it is present.

Fig. 2a shows the test accuracy of GCN with item node initialization using word vectors (left, blue bar), CORGI (middle, red bar), and GCN with edge embeddings initialized with edge labels (right, yellow bar). Unlike the last model, the first two models do not use the ground truth edge labels during training. CORGI is the only one that achieves near perfect test accuracy.

Fig. 2b and Fig. 2c illustrate the t-SNE (Van der Maaten and Hinton 2008) visualization of computed user-node and item-node embeddings for CORGI. Item and user nodes are colored by their associated content-word distributions and word-attentiveness, showing that the node embeddings can discriminate nodes by their attributes. Fig. 2d and Fig. 2e display the computed attention scores between user-item pairs for two sample pairs. When the word that the user "likes" is included in the item's associated words, CORGI correctly targets that word by assigning high attention score (Fig. 2d). When word that user "likes" is absent, the attention distribution over the content-words of an item-node becomes much more uniform.

Evaluation on real-world data

Datasets We evaluate CORGI on two real-world datasets that record different user-item interactions (Tbl. 1). The Goodreads dataset (Jannesar and Ghaderi 2020) from the Goodreads website contains users and books. The content of each book-node is its natural language description. The dataset includes a 1 to 5 integer rating between some books and users. The Eedi dataset (Wang et al. 2020) contains anonymized student and question identities with the student responses to some questions. The content of each question-node is the text of the question. Edge labels are binary: one and zero for correct and incorrect answers.

For both datasets, to encode the content within nodes in CORGI, we use a pre-trained transformer encoder model (Devlin et al. 2019) as $\mathbf{F}$. We use a *truncation threshold* T so that we ignore words that appear after T for any

$\mathbf{D}_m$ with $n(m) > T$. In our experiments, the parameters of the GNN of CORGI and the prediction multi-layer perceptron (MLP) (Eq. 8) are learned jointly during training but we do *not* fine-tune the parameters of $\mathbf{F}$. We set $T = 64$ for both Goodreads and Eedi. The appendix compares test performance with respect to varying T for Goodreads and Eedi and additional information about the dataset and the pre-processing steps.

Baselines We compare CORGI with 9 widely used missing value imputation models, discussed in related work. Deep Matrix Factorization (DMF) and Partial Variational Autoencoder (PVAE) are non-GNN matrix completion models. Graph Convolutional Network (GCN), GraphSAGE, Graph Attention Network, Jumping knowledge network, Graph isomorphism network are GNN-based models not specifically designed for recommender systems. We compare CORGI with these baselines by using a read-out MLP that accepts the concatenation of user and item node embeddings and makes a prediction for the pair, as done in Eq. 8. We also compare to graph convolutional matrix completion (GC-MC) and GRAPE (You et al. 2020) that are GNN-based models for matrix completion.

None of the previous models consider content. Thus, we consider 6 GNN node embedding initialization configurations that use content information:

GNNs with WordNodes. We create special "word nodes" for every word and connect them to a node $v_m \in \mathcal{V}_M$ if the word is contained in the item's content. This baseline allows message passing word-specific information but word ordering within item content is ignored. We retrieve words by stemming (Porter 1980), filtering non-alphanumeric words, and removing words with frequency of less than 2.

GNN Node Init: BoW is a standard GCN with the node embeddings initialized to a multi-hot bag-of-words of the content. Words are tokenized and stemmed as above.

GNN Node Init: NeuralBoW uses a pre-trained word2vec model (Mikolov et al. 2013), implemented in Gensim (Řehůřek and Sojka 2010). Words are encoded in fixed 300-dimensional vector representations and average pooling is used for node initialization.

Table 1: Dataset statistics: $|\mathcal{D}|$: Vocabulary size, $|\overline{\mathbf{D}}|$: avg num of words per item, Density: graph density, #L: num of labels.

	Nodes		Edges			Contents		Density	# L
	# Users	#Items	# Edges	/ user	/ item	$\|\mathcal{D}\|$	$\|\overline{\mathbf{D}}\|$		
Synthetic	1,000	1,000	100,000	100	100	5	2.50	0.100	2
Eedi	35,073	22,931	991,740	28	43	21,072	20.02	0.001	2
Goodreads	2,243	2,452	114,839	51	47	35,111	132.32	0.021	5

Table 2: Average test RMSE (Goodreads, lower is better) and test accuracy, AUROC, AUPR (Eedi, higher is better) results over 5 independent runs followed by one standard error. Best results are highlighted in bold, and the second-best results are underlined. $*$ and $**$ signify p-values less than 0.05 and 0.001 respectively from independent t-tests with the second-best results.

Model	Content	**Goodreads**	**Eedi**		
		RMSE ($\downarrow$)	Accuracy ($\uparrow$)	AUROC ($\uparrow$)	AUPR ($\uparrow$)
DMF (Xue et al. 2017)	✗	$0.921_{\pm 0.001}$	$0.738_{\pm 0.002}$	$0.653_{\pm 0.003}$	$0.828_{\pm 0.002}$
PVAE (Ma et al. 2019)	✗	$0.894_{\pm 0.001}$	$0.746_{\pm 0.001}$	$0.682_{\pm 0.000}$	$0.834_{\pm 0.000}$
GC-MC (Berg, Kipf, and Welling 2017)	✗	$0.916_{\pm 0.002}$	$0.735_{\pm 0.001}$	$0.672_{\pm 0.002}$	$0.819_{\pm 0.001}$
GCN (Kipf and Welling 2017)	✗	$0.893_{\pm 0.001}$	$0.746_{\pm 0.002}$	$0.680_{\pm 0.001}$	$0.830_{\pm 0.001}$
GraphSAGE (Hamilton, Ying, and Leskovec 2017)	✗	$0.898_{\pm 0.003}$	$0.742_{\pm 0.003}$	$0.665_{\pm 0.002}$	$0.838_{\pm 0.003}$
GRAPE (You et al. 2020)	✗	$0.894_{\pm 0.001}$	$0.746_{\pm 0.001}$	$0.672_{\pm 0.001}$	$0.824_{\pm 0.001}$
GAT (Veličković et al. 2018)	✗	$0.893_{\pm 0.002}$	$0.745_{\pm 0.000}$	$0.684_{\pm 0.001}$	$0.832_{\pm 0.001}$
GIN-ϵ (Xu et al. 2019)	✗	$0.892_{\pm 0.000}$	$0.747_{\pm 0.001}$	$0.689_{\pm 0.002}$	$0.838_{\pm 0.001}$
JK-LSTM (Xu et al. 2018)	✗	$0.895_{\pm 0.000}$	$0.746_{\pm 0.001}$	$0.685_{\pm 0.002}$	$0.840_{\pm 0.002}$
GCN with WordNodes	✓	$0.886_{\pm 0.002}$	$0.751_{\pm 0.002}$	$0.710_{\pm 0.002}$	$0.839_{\pm 0.003}$
GCN Init: BoW	✓	$0.891_{\pm 0.001}$	$0.748_{\pm 0.001}$	$0.710_{\pm 0.001}$	$0.836_{\pm 0.000}$
GCN Init: NeuralBoW	✓	$0.886_{\pm 0.001}$	$0.751_{\pm 0.000}$	$0.706_{\pm 0.001}$	$0.848_{\pm 0.001}$
GCN Init: BERT CLS	✓	$0.889_{\pm 0.001}$	$0.748_{\pm 0.001}$	$0.706_{\pm 0.001}$	$0.841_{\pm 0.001}$
GCN Init: BERT Avg.	✓	$0.887_{\pm 0.001}$	$0.750_{\pm 0.001}$	$0.708_{\pm 0.001}$	$0.848_{\pm 0.001}$
GCN Init: SBERT	✓	$0.890_{\pm 0.000}$	$0.752_{\pm 0.002}$	$0.708_{\pm 0.002}$	$0.848_{\pm 0.001}$
GAT Init: NeuralBoW	✓	$0.888_{\pm 0.001}$	$0.747_{\pm 0.001}$	$0.707_{\pm 0.002}$	$0.841_{\pm 0.001}$
GAT Init: BERT Avg.	✓	$0.887_{\pm 0.001}$	$0.749_{\pm 0.001}$	$0.709_{\pm 0.001}$	$0.844_{\pm 0.002}$
GAT Init: SBERT	✓	$\underline{0.884}_{\pm 0.000}$	$0.752_{\pm 0.001}$	$0.710_{\pm 0.001}$	$\underline{0.849}_{\pm 0.001}$
GRAPE Init: NeuralBoW	✓	$0.890_{\pm 0.001}$	$0.748_{\pm 0.001}$	$0.704_{\pm 0.001}$	$0.842_{\pm 0.001}$
GRAPE Init: BERT Avg.	✓	$0.889_{\pm 0.001}$	$0.749_{\pm 0.000}$	$0.704_{\pm 0.001}$	$0.838_{\pm 0.001}$
GRAPE Init: SBERT	✓	$0.892_{\pm 0.001}$	$0.750_{\pm 0.002}$	$0.711_{\pm 0.002}$	$0.846_{\pm 0.003}$
GIN Init: NeuralBoW	✓	$0.890_{\pm 0.001}$	$0.748_{\pm 0.002}$	$0.710_{\pm 0.001}$	$0.843_{\pm 0.002}$
GIN Init: BERT Avg.	✓	$0.888_{\pm 0.001}$	$0.752_{\pm 0.001}$	$\underline{0.711}_{\pm 0.001}$	$0.836_{\pm 0.002}$
GIN Init: SBERT	✓	$0.885_{\pm 0.000}$	$\underline{0.752}_{\pm 0.000}$	$0.711_{\pm 0.000}$	$0.845_{\pm 0.001}$
JK Init: NeuralBoW	✓	$0.889_{\pm 0.000}$	$0.747_{\pm 0.002}$	$0.709_{\pm 0.001}$	$0.842_{\pm 0.000}$
JK Init: BERT Avg.	✓	$0.889_{\pm 0.001}$	$0.749_{\pm 0.002}$	$0.708_{\pm 0.001}$	$0.838_{\pm 0.001}$
JK Init: SBERT	✓	$0.886_{\pm 0.000}$	$0.751_{\pm 0.001}$	$0.710_{\pm 0.001}$	$0.839_{\pm 0.002}$
CORGI: Concat	✓	$\mathbf{0.873}^{**}_{\pm 0.000}$	$\mathbf{0.761}^{**}_{\pm 0.001}$	$\mathbf{0.720}^{**}_{\pm 0.001}$	$\mathbf{0.891}^{**}_{\pm 0.000}$
CORGI: Dot-product	✓	$\mathbf{0.872}^{**}_{\pm 0.000}$	$\mathbf{0.760}^{**}_{\pm 0.001}$	$\mathbf{0.721}^{**}_{\pm 0.001}$	$\mathbf{0.888}^{**}_{\pm 0.001}$

GNN Node Init: BERT CLS uses pre-trained, cased BERT-base (Devlin et al. 2019), impemented in Hugging-Face (Wolf et al. 2019). Words are encoded in 768-dimensional vector representations. and the representation of `[CLS]` is used to initalize node embeddings.

GNN Node Init: BERT Avg uses identical settings as above, but instead of the `[CLS]` token, we use average pooling over all the output vector representations.

GNN Node Init: SBERT uses the 768-dimensional vector representations encoding of the whole document with the SBERT model of Reimers et al. (2019).

In all cases, the content vector is mapped to the initial node embeddings using a learned linear layer.

Missing value imputation Tbl. 2 compares the missing value imputation performance on the Goodreads and Eedi datasets over 5 runs. We report root mean square error (RMSE) for Goodreads and accuracy, area under the receiver operating characteristic (AUROC), and area under the precision-recall curve (AUPR) for Eedi. Overall, we observe improved performance when node content is used. Compared to the baseline models with content, both CORGI constructions (concatenation and dot-product) outperform baselines on both datasets with statistical significance.

Fig. 3 shows the content attention distributions of user

Table 3: Mean $\pm$ one standard error of rating prediction over 5 runs (Goodreads, test RMSE) and response prediction (Eedi, test accuracy) results of all users (All), users with node degree greater than 10 ($D > 10$), and users with degrees less than or equal to 10 ($D \leq 10$). $*$ and $**$ signify p-values less than 0.05 and 0.001 respectively from paired t-tests.

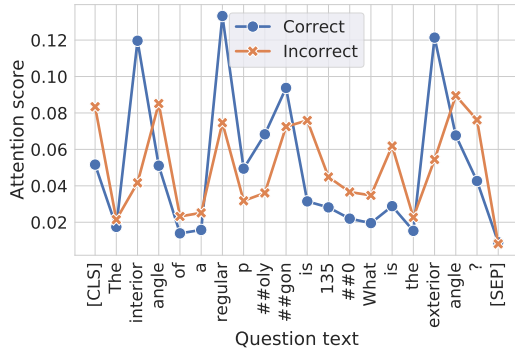|	Goodreads - RMSE ($\downarrow$)			Eedi - Accuracy ($\uparrow$)		
	All	$D > 10$	$D \leq 10$	All	$D > 10$	$D \leq 10$
GCN	$0.792_{\pm 0.007}$	$0.796_{\pm 0.008}$	$0.752_{\pm 0.03}$	$0.746_{\pm 0.002}$	$0.751_{\pm 0.002}$	$0.720_{\pm 0.008}$
GCN N.I.: SBERT	$0.786_{\pm 0.006}$	$0.789_{\pm 0.007}$	$0.728_{\pm 0.03}$	$0.753_{\pm 0.003}$	$0.757_{\pm 0.002}$	$0.727_{\pm 0.008}$
CORGI (DP)	$\mathbf{0.781}^*_{\pm 0.006}$	$\mathbf{0.786}_{\pm 0.007}$	$\mathbf{0.685}^{**}_{\pm 0.03}$	$\mathbf{0.758}^*_{\pm 0.002}$	$\mathbf{0.760}^*_{\pm 0.003}$	$\mathbf{0.750}^{**}_{\pm 0.010}$

Figure 3: Example content attention distributions of students with correct and incorrect answers.
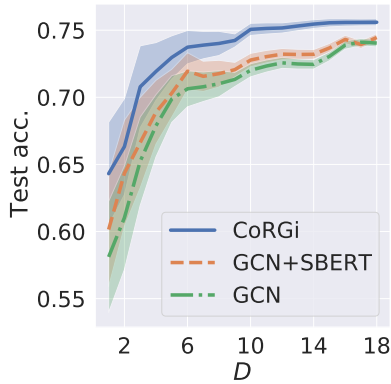

Figure 4: Test accuracy vs. user node degree for Eedi.

(student) - item (question) pairs in Eedi dataset for a particular question. The blue circle line shows the average attention scores of students who got the question right, and the orange cross line shows that of students with incorrect answers. We observe *user-item-specific* attention scores assigned; the student with right answer has high attention scores for tokens interior, regular, and exterior, while the student with wrong answer attends more to tokens angle, angle, and [CLS]. This is in contrast to baselines that exploit the content information of items in a way that does not explicitly distinguish users during the message passing.

Sparsity analysis Finally, we test the hypothesis that content is particularly useful in sparse — less connected — regions of the recommendation. Tbl. 3 shows rating and re-

Table 4: Win rates (column vs. row) in inductive setting for two held-out rates (0.5 and 0.99).

	GRAPE	Init: SBERT
Init: SBERT	0.514 / 0.610	-
CORGI	0.532 / 0.837	0.526 / 0.695

sponse prediction performance on Goodreads and Eedi vs. the user node degree (D), , i.e., the number of questions answered or books rated. CORGI outperforms the baselines with $p < 0.05$ from paired t-tests with respect to GCN Node Init: SBERT. On both datasets, the predictive performance between CORGI and the comparison models is relatively comparable for users that have interacted with more items ($D > 10$), although CORGI still outperforms them. On the contrary, the difference in performance between CORGI and the comparison models becomes more significant for users connected with $D \leq 10$, showing the effectiveness of CORGI. Fig. 4 shows test accuracy on Eedi with varying degrees, showing an increasing gap between CORGI and baselines with smaller Ds.

Tbl. 4 show the relative predictive performance of CORGI over the comparison models in inductive settings, i.e., prediction on users that were not seen during training but newly introduced during inference, in the Eedi dataset. We evaluate win-rate, the rate at which a model's prediction is correct and the other model's prediction is wrong. We find that when the train graph becomes sparse with larger number of unseen nodes during training, CORGI's relative predictive performance compared to the baseline models improves compared to the dense setting.

Conclusion

We presented CORGI, a message-passing GNN that tightly integrates node content using attention. Using node content — such as text — allows us to capture rich information within the modeled domain while exploiting the structured form of the data. This is particularly evident in sparse regions of graphs. Future work may further investigate how non-text modalities can be captured in content-rich graphs across a range of applications beyond edge value prediction.

References

Bennett, J.; Lanning, S.; et al. 2007. The Netflix prize. In *Proceedings of KDD cup and workshop*, volume 2007, 35.

Berg, R. v. d.; Kipf, T.; and Welling, M. 2017. Graph convolutional matrix completion. In *KDD Deep Learning Day Workshop*.

Billsus, D.; Pazzani, M.; et al. 1998. Learning collaborative information filters. In *ICML*.

Bojanowski, P.; Grave, E.; Joulin, A.; and Mikolov, T. 2017. Enriching word vectors with subword information. *TACL*, 5: 135–146.

Bruna, J.; Zaremba, W.; Szlam, A.; and LeCun, Y. 2013. Spectral networks and locally connected networks on graphs. *arXiv preprint arXiv:1312.6203*.

Cho, K.; van Merrienboer, B.; Gülçehre, Ç.; Bahdanau, D.; Bougares, F.; Schwenk, H.; and Bengio, Y. 2014. Learning Phrase Representations using RNN Encoder-Decoder for Statistical Machine Translation. In *EMNLP*.

Defferrard, M.; Bresson, X.; and Vandergheynst, P. 2016. Convolutional neural networks on graphs with fast localized spectral filtering. In *NeurIPS*.

Devlin, J.; Chang, M.-W.; Lee, K.; and Toutanova, K. 2019. BERT: Pre-training of Deep Bidirectional Transformers for Language Understanding. In *NAACL*.

Duvenaud, D.; Maclaurin, D.; Aguilera-Iparraguirre, J.; Gómez-Bombarelli, R.; Hirzel, T.; Aspuru-Guzik, A.; and Adams, R. 2015. Convolutional networks on graphs for learning molecular fingerprints. In *NeurIPS*.

Gao, H.; and Ji, S. 2019. Graph representation learning via hard and channel-wise attention networks. In *KDD*.

Gilmer, J.; Schoenholz, S.; Riley, P.; Vinyals, O.; and Dahl, G. 2017. Neural message passing for quantum chemistry. In *ICML*.

Grover, A.; and Leskovec, J. 2016. node2vec: Scalable feature learning for networks. In *KDD*.

Hamilton, W. L.; Ying, R.; and Leskovec, J. 2017. Inductive representation learning on large graphs. In *NeurIPS*.

He, X.; Deng, K.; Wang, X.; Li, Y.; Zhang, Y.; and Wang, M. 2020. Lightgcn: Simplifying and powering graph convolution network for recommendation. In *SIGIR*.

Hou, Y.; Zhang, J.; Cheng, J.; Ma, K.; Ma, R. T.; Chen, H.; and Yang, M.-C. 2020. Measuring and improving the use of graph information in graph neural networks. In *ICLR*.

Jannesar, B.; and Ghaderi, S. 2020. Goodreads book dataset. https://github.com/BahramJannesar/GoodreadsBookDataset.

Kim, D.; and Oh, A. 2021. How to Find Your Friendly Neighborhood: Graph Attention Design with Self-Supervision. In *ICLR*.

Kingma, D.; and Ba, J. 2014. Adam: A method for stochastic optimization. In *ICLR*.

Kingma, D.; and Welling, M. 2014. Auto-encoding variational Bayes. In *ICLR*.

Kipf, T.; and Welling, M. 2017. Semi-supervised classification with graph convolutional networks. In *ICLR*.

Koren, Y.; Bell, R.; and Volinsky, C. 2009. Matrix factorization techniques for recommender systems. *Computer*, 42(8): 30–37.

Li, Y.; Tarlow, D.; Brockschmidt, M.; and Zemel, R. 2016. Gated graph sequence neural networks. In *ICLR*.

Lin, Z.; Feng, M.; Santos, C. N. d.; Yu, M.; Xiang, B.; Zhou, B.; and Bengio, Y. 2017. A structured self-attentive sentence embedding. In *ICLR*.

Linden, G.; Smith, B.; and York, J. 2003. Amazon. com recommendations: Item-to-item collaborative filtering. *IEEE Internet Computing*, 7(1): 76–80.

Ma, C.; Tschiatschek, S.; Palla, K.; Hernandez-Lobato, J. M.; Nowozin, S.; and Zhang, C. 2019. EDDI: Efficient Dynamic Discovery of High-Value Information with Partial VAE. In *ICML*.

McAuley, J.; and Leskovec, J. 2013. Hidden factors and hidden topics: understanding rating dimensions with review text. In *RecSys*.

Mikolov, T.; Sutskever, I.; Chen, K.; Corrado, G.; and Dean, J. 2013. Distributed representations of words and phrases and their compositionality. In *NeurIPS*.

Mnih, A.; and Salakhutdinov, R. 2007. Probabilistic matrix factorization. In *NeurIPS*.

Nair, V.; and Hinton, G. 2010. Rectified linear units improve restricted Boltzmann machines. In *ICML*.

Niepert, M.; Ahmed, M.; and Kutzkov, K. 2016. Learning convolutional neural networks for graphs. In *ICML*.

Parikh, A.; Täckström, O.; Das, D.; and Uszkoreit, J. 2016. A Decomposable Attention Model for Natural Language Inference. In *EMNLP*.

Paulus, R.; Xiong, C.; and Socher, R. 2018. A Deep Reinforced Model for Abstractive Summarization. In *ICLR*.

Pennington, J.; Socher, R.; and Manning, C. 2014. Glove: Global vectors for word representation. In *EMNLP*.

Perozzi, B.; Al-Rfou, R.; and Skiena, S. 2014. Deepwalk: Online learning of social representations. In *KDD*.

Peters, M.; Neumann, M.; Iyyer, M.; Gardner, M.; Clark, C.; Lee, K.; and Zettlemoyer, L. 2018. Deep Contextualized Word Representations. In *NAACL*.

Porter, M. F. 1980. An algorithm for suffix stripping. *Program*, 14(3): 130–137.

Řehůřek, R.; and Sojka, P. 2010. Software Framework for Topic Modelling with Large Corpora. In *Proceedings of the LREC 2010 Workshop on New Challenges for NLP Frameworks*. http://is.muni.cz/publication/884893/en.

Reimers, N.; Gurevych, I.; Reimers, N.; Gurevych, I.; Thakur, N.; Reimers, N.; Daxenberger, J.; and Gurevych, I. 2019. Sentence-BERT: Sentence Embeddings using Siamese BERT-Networks. In *EMNLP*.

Sarwar, B.; Karypis, G.; Konstan, J.; and Riedl, J. 2001. Item-based collaborative filtering recommendation algorithms. In *WWW*.

Scarselli, F.; Gori, M.; Tsoi, A. C.; Hagenbuchner, M.; and Monfardini, G. 2008. The graph neural network model. *IEEE Transactions on Neural Networks*, 20(1): 61–80.

Spinelli, I.; Scardapane, S.; and Uncini, A. 2020. Missing data imputation with adversarially-trained graph convolutional networks. *Neural Networks*, 129: 249–260.

Srivastava, N.; Hinton, G.; Krizhevsky, A.; Sutskever, I.; and Salakhutdinov, R. 2014. Dropout: a simple way to prevent neural networks from overfitting. *JMLR*, 15(1): 1929–1958.

Sutskever, I.; Vinyals, O.; and Le, Q. 2014. Sequence to sequence learning with neural networks. In *NeurIPS*.

Tang, J.; Qu, M.; Wang, M.; Zhang, M.; Yan, J.; and Mei, Q. 2015. Line: Large-scale information network embedding. In *WWW*.

Van der Maaten, L.; and Hinton, G. 2008. Visualizing data using t-SNE. *JMLR*, 9(11).

Vaswani, A.; Shazeer, N.; Parmar, N.; Uszkoreit, J.; Jones, L.; Gomez, A.; Kaiser, L.; and Polosukhin, I. 2017. Attention is All you Need. In *NeurIPS*.

Veličković, P.; Cucurull, G.; Casanova, A.; Romero, A.; Lio, P.; and Bengio, Y. 2018. Graph attention networks. In *ICLR*.

Vincent, P.; Larochelle, H.; Bengio, Y.; and Manzagol, P.-A. 2008. Extracting and composing robust features with denoising autoencoders. In *ICML*.

Wang, X.; He, X.; Wang, M.; Feng, F.; and Chua, T.-S. 2019. Neural graph collaborative filtering. In *SIGIR*.

Wang, Z.; Lamb, A.; Saveliev, E.; Cameron, P.; Zaykov, Y.; Hernández-Lobato, J. M.; Turner, R. E.; Baraniuk, R. G.; Barton, C.; Jones, S. P.; et al. 2020. Diagnostic questions: The NeurIPS 2020 education challenge. *arXiv preprint arXiv:2007.12061*.

Wolf, T.; Debut, L.; Sanh, V.; Chaumond, J.; Delangue, C.; Moi, A.; Cistac, P.; Rault, T.; Louf, R.; Funtowicz, M.; et al. 2019. HuggingFace's Transformers: State-of-the-art natural language processing. *arXiv preprint arXiv:1910.03771*.

Wu, S.; Sun, F.; Zhang, W.; and Cui, B. 2020. Graph neural networks in recommender systems: a survey. *arXiv preprint arXiv:2011.02260*.

Xu, K.; Hu, W.; Leskovec, J.; and Jegelka, S. 2019. How Powerful are Graph Neural Networks? In *ICLR*.

Xu, K.; Li, C.; Tian, Y.; Sonobe, T.; Kawarabayashi, K.-i.; and Jegelka, S. 2018. Representation learning on graphs with jumping knowledge networks. In *ICML*.

Xue, H.-J.; Dai, X.; Zhang, J.; Huang, S.; and Chen, J. 2017. Deep Matrix Factorization Models for Recommender Systems. In *IJCAI*.

Yoon, J.; Jordon, J.; and Schaar, M. 2018. Gain: Missing data imputation using generative adversarial nets. In *ICML*.

You, J.; Ma, X.; Ding, D. Y.; Kochenderfer, M.; and Leskovec, J. 2020. Handling missing data with graph representation learning. In *NeurIPS*.

You, Y.; Jia, W.; Liu, T.; and Yang, W. 2019. Improving abstractive document summarization with salient information modeling. In *ACL*.

Zhang, J.; Shi, X.; Xie, J.; Ma, H.; King, I.; and Yeung, D.-Y. 2018. GaAN: Gated attention networks for learning on large and spatiotemporal graphs. *arXiv preprint arXiv:1803.07294*.

Zhang, M.; and Chen, Y. 2020. Inductive Matrix Completion Based on Graph Neural Networks. In *ICLR*.

Summary of key notations used in the paper

We summarize the key notations used throughout the paper. We group notations in three groups: (a) notations on graph sets and the corresponding elements. (b) variables and parameters used to describe the forward pass of CORGI. (c) notations used to describe the content information associated to content or item nodes.

In addition to this, we have the trainable weights explained during the message passing of CORGI: $\mathbf{P}^{(l)}$ and $\mathbf{Q}^{(l)}$ for updating node embeddings, $\mathbf{W}_U^{(l)}$, $\mathbf{W}_M^{(l)}$, and $\mathbf{p}^{(l)}$ for computing attention coefficients, and $\mathbf{w}_{\text{out}}$ and b for the prediction MLP.

Table 5: Key notations used in the paper.

	Symbols	Description
Graph sets & elements	$\mathcal{V}$	The set of all nodes in the graph
	$\mathcal{V}_C, \mathcal{V}_M, \mathcal{V}_U \subset \mathcal{V}$	The sets of content, item, and user nodes
	$\mathcal{E}$	The set of all edges in the graph
	$\mathcal{N}(i)$	Neighborhood function for node v_i
CORGI variables	$\mathbf{h}_i^{(0)}$	Input feature of node v_i of size $C^{(l,h)}$
	$\mathbf{e}_{ij}^{(0)}$	Input feature of edge e_{ij} of size $C^{(l,e)}$
	$\mathbf{h}_i^{(l)}$	Node embedding of v_i at l^{th} layer
	$\mathbf{e}_{ij}^{(l)}$	Edge embedding between v_i and v_j at l^{th} layer
	$\mathbf{e}_{ij}^{(l)\prime}$	Edge embedding before content update
	$\mathbf{e}_{ij,\mathrm{CA}}^{(l)}$	Edge embedding from content-attention
	$c_{ik}^{(l)}$	Attention coefficient between v_i and content k
	$\alpha_{ik}^{(l)}$	Attention probability from $c_{ik}^{(l)}$ after SOFTMAX
Content-related notations	$n(i)$	The number of content vectors associated to v_i
	$\mathbf{Z}_i = \{\mathbf{z}_k^{(i)}\}_1^{n(i)} \subset \mathbb{R}^D$	A set of content vectors associated to v_i
	$\mathbf{D}_i = [w_1^{(i)}, \cdots, w_{n(i)}^{(i)}]$	A sequence of words associated to v_i
	$\mathbf{F}$	A sequence encoder that projects $\mathbf{D}_i$ to $\mathbf{Z}_i$

Additional experiments
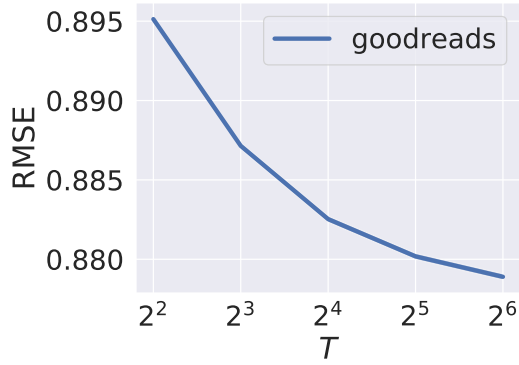
Truncation threshold and test performance

Figure 5: Truncation size and test accuracy for the Goodreads dataset. Note semi-log-x and starting point for y-axis.
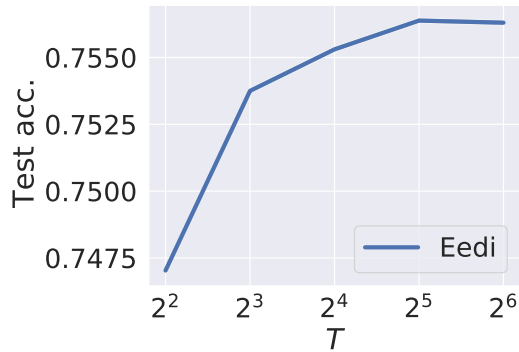

Figure 6: Truncation size and RMSE for the Eedi dataset. Note semi-log-x and starting point for y-axis.

We test the affect of the truncation threshold T on the test performance. In sequential content encoders $\mathbf{F}$ such as the transformer encodes $\mathbf{D_m}$, i.e., the contents of an item node v_m of size $n(m)$ into a set of content vector representations $\mathbf{Z}_m$. During encoding, if $n(m)$ is greater than the truncation threshold T, we only the first T words only, i.e., $|\mathbf{Z}_m| = \min(n(m), T)$. Setting T to a high value enables CORGI to fully exploit the content information, at a trade-off that makes the models slow to train with larger memory requirement.

Fig. 5 and 6 show the test performance with respect to varying values of T on the Goodreads and Eedi datasets. For both datasets, increasing T results in higher test performance (T greater than 64 results in the memory error on our computing infrastructure). The average number of words on Eedi questions 20.02 (Tbl. 1), and the test performance converges at $T = 32$. On the other hand, the average number of words on Goodreads book descriptions is 132.32, and we observe that the test performance does not fully converge at $T = 64$.

Table 6: Performance comparison with and without the caching trick on Goodreads dataset.

	RMSE	Training time / iteration (sec.)
With caching	$0.879_{\pm 0.000}$	10.41
Without caching	$0.879_{\pm 0.000}$	41.86

Performance comparison on caching trick

In Sec. 10, we introduce a caching trick that allows the reduction in training time and memory requirement. Specifically, the caching trick is realized by creating a cache for $\mathbf{e}_{ij,\mathrm{CA}}^{(l)}$ with zero initializations. We then update at the final layer L only, by computing $\mathbf{e}_{ij,\mathrm{CA}}^{(L)}$ using Eq. 4 and updating the cache for all $\mathbf{e}_{ij,\mathrm{CA}}^{(l)}$ to the computed $\mathbf{e}_{ij,\mathrm{CA}}^{(L)}$. Using the caching trick along with the neighbor sampling (Hamilton, Ying, and Leskovec 2017), the time complexity reduces from

$$\mathcal{O}\Big(|\mathcal{V}_U| \cdot C^{(l-1,h)} \cdot C^{(l,e)} + |\mathcal{V}_M| \cdot T \cdot D \cdot C^{(l,e)} + |\mathcal{E}| \cdot T \cdot C^{(l,e)}\Big)$$

to

$$\mathcal{O}\Big(|\mathcal{N}(\mathcal{V}'_M)| \cdot C^{(l-1,h)} \cdot C^{(l,e)} + |\mathcal{V}'_M| \cdot T \cdot D \cdot C^{(l,e)} + |\mathcal{E}'| \cdot T \cdot C^{(l,e)}\Big),$$

where we sample a subset of nodes $\mathcal{V}' = \big\{\mathcal{V}'_U \cup \mathcal{V}'_M\big\}$ for the neighbor sampling and only update $\mathbf{e}_{ij,\mathrm{CA}}$ whose target node v_j is in $\mathcal{V}'_M$ and source node v_i is in $\mathcal{N}(\mathcal{V}'_M)$.

Tbl. 6 compares the predictive performance of CORGI with and without the caching trick on Goodreads dataset in terms of RMSE and wall-clock training time. The predictive performance comparison on Eedi dataset was not feasible due to excessive memory requirement in the absence of the caching trick. In the absence of the caching trick, the predictive performance remains the same, but the training time is increased more than 4 times per iteration.

Table 7: Comparison of different combination methods for updating the edge embedding $\mathbf{e}_{ij}^{(l)}$ on the Goodreads dataset. We report RMSE (lower the better).

Combination method	CORGI :Concat	CORGI :Dot-product
$\mathbf{e}_{ij}^{(l)\prime} + \mathbf{e}_{ij,\text{CA}}^{(l)}$	$0.879_{\pm 0.000}$	$0.879_{\pm 0.000}$
$\text{CONCAT}(\mathbf{e}_{ij}^{(0)}, \mathbf{e}_{ij,\text{CA}}^{(l)})$	$0.886_{\pm 0.000}$	$0.884_{\pm 0.001}$

Table 8: Comparison of different combination methods for updating the edge embedding $\mathbf{e}_{ij}^{(l)}$ on the Eedi dataset. We report test accuracy (higher the better).

Combination method	CORGI :Concat	CORGI :Dot-product
$\mathbf{e}_{ij}^{(l)\prime} + \mathbf{e}_{ij,\text{CA}}^{(l)}$	$0.756_{\pm 0.001}$	$0.757_{\pm 0.001}$
$\text{CONCAT}(\mathbf{e}_{ij}^{(0)}, \mathbf{e}_{ij,\text{CA}}^{(l)})$	$0.752_{\pm 0.001}$	$0.752_{\pm 0.001}$

Comparison on different combination methods

In Sec. we introduce two ways to augment the computed content-attention (CA) edge embeddings $\mathbf{e}_{ij,\text{CA}}^{(l)}$ to edge embeddings $\mathbf{e}_{ij}^{(l)}$ between nodes v_i and v_j at l^{th} layer. The first method is to first update the edge embeddings without the content attention $(\mathbf{e}_{ij}^{(l)\prime})$ and use the element-wise addition. The second method is to concatenate with the input edge feature $\mathbf{e}_{ij}^{(0)}$. We compare the predictive performances of these methods for the Goodreads and Eedi datasets. In Tables 7 and 8, element-wise addition yields better predictive performance than concatenation for on both datasets with varying methods of attention computation: concat and dot-product.

Bi-directional setting for CORGI

In the formulation introduced in Eq. 4, the computation of the content attention vector is skipped when the target node is an item and the source node is a user. In fact, CORGI works in more general settings than the recommendation system, where every node can potentially be associated with contents. However, in a recommendation system with bipartite graphs, it is common that only item nodes are associated with such content information. We have made a change in this formulation so that the update of the content attention (CA) vector is now bi-directional, e.g., whenever gets updated, update in the same fashion instead of skipping. In Tables 9 and 10, we report results when the update of CA edge representation is bi-directional by simultaneously updating both from i to j and j to i edges. The results show the significant improvement in the predictive performance.

Additional details on model training

Datasets

Here, we provide additional information about the two real-world datasets used in our experiment. We chose the Goodreads and Eedi datasets because they contains text information in sentences associated with each item.

We use Goodreads dataset from Jannesar and Ghaderi (2020). We filtered out books whose descriptions are written in non-English languages, and removed duplicate books based on their titles. Originally, the ratings were text-based. We converted the ratings as follows: "Did not like it" to rating 1, "It was okay" to rating 2, "Liked it" to rating 3, "Really liked it" to rating 4, and "It was amazing" to rating 5.

We used Eedi dataset from Wang et al. (2020). The content of the text information is extracted using optical character recognition (OCR) from the raw question images, as no question text is available.

In order to train CORGI and comparison models on a single GPU within our computation infrastructure, we took a subset of the Eedi dataset, taking student responses from between March 4th and March 27th.

Configurations for the baseline methods

We detail the configurations used specific to each baseline for recording the test performance. For GC-MC, we assign the separate message passing channels and their corresponding parameters for modeling different discrete edge labels. The number of layer is set to 1, and We do not use the weight sharing method. For the accumulation method, we use concatenation. For GraphSAGE, we use the neighbor sampling size of 32 throughout all message passing layers. For GRAPE, we do not use the one-hot node initializations for both Eedi and Goodreads, because of the large number of item nodes leading to GPU memory errors. Instead, we use random initialization just like all GNN model configurations in our experiment. For GAT, we use a single self-attention head. Alternatively, we also tested using multi-head attention with 4 heads with smaller $C^{(l,h)} = 16$, but the predictive performance did not increase. We could not test multi-head attention with $C^{(l,h)} = 64$ due to the GPU memory limits. For GIN, we make the epsilon parameter trainable (Noted as GIN-ϵ in the original GIN paper). For JK, we choose LSTM during aggregation (Noted as JK-LSTM in the original JK paper). Both settings have shown to perform best amongst all configurations in the respective papers.

Computing infrastructure

Each experiment was run on a single GPU, which was either an NVIDIA Tesla K80 or an NVIDIA Tesla V100. All experiments were scheduled and performed in Azure Machine Learning.

Table 9: Predictive performance of CORGI for bidirectional setting when concatenation is used for attention computation.

Concat	Goodreads	EEDI		
	RMSE (↓)	Accuracy (↑)	AUROC (↑)	AUPR (↑)
User-only	0.879 ± 0.000	0.756 ± 0.002	0.715 ± 0.002	0.874 ± 0.002
Bidirectional	$\mathbf{0.873}\pm0.001$	$\mathbf{0.761}\pm0.001$	$\mathbf{0.720}\pm0.002$	$\mathbf{0.891}\pm0.001$

Table 10: Predictive performance of CORGI for bidirectional setting when dot-product is used for attention computation.

Dot-product	Goodreads	EEDI		
	RMSE (↓)	Accuracy (↑)	AUROC (↑)	AUPR (↑)
User-only	0.879 ± 0.001	0.757 ± 0.001	0.717 ± 0.001	0.874 ± 0.001
Bidirectional	$\mathbf{0.872}\pm0.001$	$\mathbf{0.760}\pm0.002$	$\mathbf{0.721}\pm0.002$	$\mathbf{0.888}\pm0.001$